

5 Building microclimate and summer thermal comfort in free-running buildings with diverse spaces

a Chinese vernacular house case⁴

ABSTRACT In this paper, the authors first clarify the definition of building microclimate in free-running buildings and the relationship with summer thermal comfort. Next, field measurements were conducted to investigate the microclimate in a Chinese traditional vernacular house. Subsequently, the results of measurements were compared with a dynamic thermal and a CFD simulation in order to determine the

⁴ This chapter is the original version which is published as: Du, X., Bokel, R., & van den Dobbelsteen, A. (2014). Building microclimate and summer thermal comfort in free-running buildings with diverse spaces: A Chinese vernacular house case. *Building and Environment*, 82, 215-227. doi: 10.1016/j.buildenv.2014.08.022

building microclimate and thermal comfort of the present vernacular house over the period of an entire summer. The field measurements show the present Chinese vernacular house has its own independent building microclimate in summer, which is in accordance with the main character of microclimate in terms of different distributions of solar gain, air temperature and wind velocity in different spaces. The simulation results of the vernacular house could be matched well with the field measurements. According to the simulations, at night, a comfortable temperature could be obtained throughout most of the summer period whereas in the daytime the operative temperature was higher than the comfortable temperature for one-third of the summer period. Wind velocity in the semi-outdoor and outdoor spaces however, improves the thermal comfort significantly. The thermal comfort environment can thus not only change in time but also in space. This example of the vernacular building shows that it is possible to create comfortable conditions for the inhabitants when not only the indoor climate is taken into account but the whole building microclimate as defined in this paper. This paper also shows that the simulations can predict the building microclimate.

KEYWORDS Building microclimate, Summer thermal comfort, Adaptive thermal comfort, Free-running building, Diverse spaces, Chinese vernacular house

5.1 Introduction

In recent years, researchers, environmentalists and architects have become increasingly interested in the thermal performance of buildings in summer. This interest is mainly directed at the two main aspects, energy consumption and thermal comfort. Rising standards of living, the globalization of modern architecture, urban heat islands and global climate change, together with the affordability of air conditioning, have caused the energy demand for cooling to increase dramatically. Studies have shown that refrigeration and air conditioning are responsible for about 15% of the total electricity consumption in the world (Santamouris & Kolokotsa, 2013). On the other hand, the thermal comfort in modern buildings, whether free-running or air-conditioned, tends to be poor. Inferior architectural design can make it impossible to utilize passive cooling approaches for thermal comfort in summer, while the constant use of air conditioning leads to uncomfortable conditions due to the bad indoor environmental quality.

Climatic features can significantly influence the performance of the built environment in terms of thermal comfort and energy consumption. When spatial scale is considered, the climate can be subdivided into macro-scale, meso-scale, local scale and micro-scale (Oke, 1987). There is no strict boundary between the different scales. For urban planning and architectural design, local climate and microclimate are the main focus.

Bioclimatic design is an approach based on local climate. These methods result in buildings that respond to the climatic conditions of their environment, are able to modify them and thus contribute to resource conservation with maximum comfort (Zuhairy & Sayigh, 1993). The design of the built environment can modify the climate on different scales, especially the microclimate scale. Hence, in bioclimatic building design in which passive approaches are applied, it is crucial to first analyse the local climate and microclimate to which the building is exposed and to explore how the microclimate can be modified and improved to ensure a good building performance.

Neither the horizontal extent nor the vertical thickness of the air layer of the microclimate is rigidly defined, although several millimetres to 1 kilometre is often employed (Oke, 1987). Within a particular region, deviations in the climate are experienced from place to place within a few kilometres distance, forming a small-scale pattern of climate, called the microclimate (M. Santamouris & Asimakopoulos, 1996). With respect to urban and building design, neighbourhood, urban canyon, building block, building and indoor space are all part of the microclimate spatial scale. In the microclimate, the distribution of air temperature, relative humidity, solar radiation and wind characteristics are the principal elements determining the physical character of the microclimate.

A literature review revealed that the majority of previous studies have focused on the urban microclimate in relation to the urban scale, i.e., neighbourhoods, urban canyons and building blocks. Some researchers have conducted field studies on the thermal environment, assessing aspects such as air temperature distribution and wind characteristics in the urban microclimate (urban canyon and streets) (Dimoudi, Kantzioura, Zoras, Pallas, & Kosmopoulos, 2013; Gaitani et al., 2011; Niachou et al., 2008). Others have examined the effect of geometry and orientation on urban and street canyon (Andreou, 2014; Giannopoulou et al., 2010; Shashua-Bar & Hoffman, 2003; Zhen, & Jiasong, 2006). Still other researchers have studied the thermal comfort of outdoor and semi-outdoor environments in the urban microclimate (Andreou, 2013; Ali-Toudert et al., 2005; Spagnolo & de Dear, 2003; Taleghani, Kleerekoper, Tenpierik, & van den Dobbelsteen, 2014). Studies have also been carried out to investigate how to use passive approaches to improve the thermal comfort of outdoor spaces (Al-Sallal & Al-Rais, 2012; Gaitani, Mihalakou,

& Santamouris, 2007; Santamouris et al., 2012; Shashua-Bar, Tsiros, & Hoffman, 2012). On the other hand, large number of studies focused on indoor climate. Few studies focused on the microclimate at the single building scale.

In this paper, the authors first clarify the definition of building microclimate in free-running buildings and define the building microclimate in terms of building spatial features, thermo-physical features and the relationship with summer thermal comfort. Next, the authors discuss the field measurements conducted to investigate the microclimate in a Chinese traditional vernacular house. This house is free-running, comprises of a number of different spaces and is situated in a hot and humid summer climate region of China. Subsequently, the results of measurements were compared with a dynamic thermal and a CFD simulation in order to determine the microclimate and thermal comfort of the typical Chinese vernacular house over the period of an entire summer. The authors expect their findings to contribute to more comfortable and more energy-efficient buildings using bioclimatic design in hot and humid summer climates.

5.2 Building microclimate and thermal comfort

In this section, the authors clarify the definition of building microclimate, as used in this paper. The authors also attempt to clarify the relationship between building microclimate and summer thermal comfort in the free-running buildings.

5.2.1 Building microclimate

As mentioned above, the term microclimate in urban planning and urban design always refers to the climate connected with a group of buildings in the urban fabric or to the climate around a single building. But, within a particular building, a small-scale pattern of “building microclimate” is found, which is different from the microclimate related to the urban fabric scale. In this paper, “building microclimate” refers to one type of microclimate, involving the indoor space and the spaces around the indoor spaces of a particular building. It is the extension of the indoor

climate. The building microclimate is mainly defined by the spatial and the thermo-physical properties.

The spatial characteristics of a building microclimate regard the following aspects (Figure 5.1):

The spatial scale is smaller than the urban fabric. It rarely covers an area more than several hundred meters wide, but is bigger than an indoor space alone. It is limited to one particular building, whether a small house or a big stadium.

The spaces in a building microclimate are connected for particular building functions in one building. The spaces are connected either directly or by building components such as walls, roofs and beams. Sometimes, the area of an urban canyon or building block is similar in size to one big single building. However, urban canyons and building blocks lack continuous spaces for particular building functions. Architectural decisions are typically made at the building scale, thus effect the building microclimate.

The existence of diverse types of spaces is another important feature of the building microclimate, distinguishing it from a single indoor climate. Indoor space, semi-outdoor space and outdoor space are the main spatial types in a building microclimate. Hence corridors, semi-outdoor rooms, courtyards, patios and atria play a very important role in the spatial design to obtain a good building microclimate.

The boundary between the different spaces should be adaptive and switchable. For example, the openable windows and doors in the boundaries always are adaptive. This applies especially to the boundary between the indoor space and the semi-outdoor space and outdoor space. As a result, the spaces can be mutually adjusted as needed.

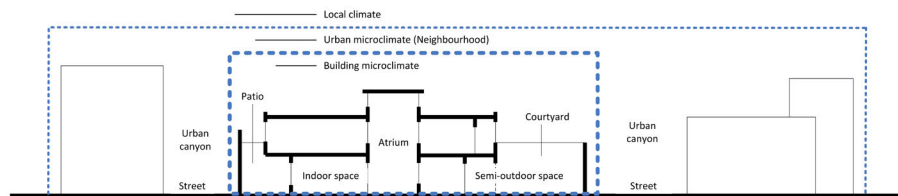


FIG. 5.1 The spatial features of building microclimate

At the building microclimate scale, the thermo-physical properties are as follows:

The average air temperature and humidity in the building microclimate are influenced by the local climate. However, air temperature and humidity distribution vary in the different spatial types. In summer, normally, the indoor temperature of the free-running buildings is lower than the semi-outdoor and outdoor temperature during the daytime; at night, the situation is reversed. The humidity follows the air temperature changes.

The influence of the local climate on the solar radiation in the microclimate is relatively small, but is significantly influenced by the design of the building components.

The wind velocity distribution is significantly different in different spaces. Generally, the wind velocity in the semi-outdoor and outdoor space is higher than in indoor spaces. The wind velocity and direction are influenced by the local wind environment, the organization of building spaces and the envelope design.

5.2.2 Thermal comfort in a building microclimate

In the building microclimate identified above, the spatial features and thermal properties of the building microclimate are interactive, just as in the urban space, where urban form, landscape and used material influence the urban microclimate. Similarly, the building microclimate is significantly influenced by building form, spatial organization, vegetation and landscape in building and construction materials. The essence of architectural bioclimatic design is to understand the local climate and utilize appropriate design strategies for building form generation and material selection, in order to create or modify the building microclimate required for a comfortable living environment. Building form, solar control and natural ventilation are the main bioclimatic design strategies to control the building microclimate. In this paper, the authors will explain the relationship between building microclimate and summer thermal comfort using adaptive thermal comfort theory. Architectural bioclimatic design strategies for modifying the building microclimate will be in the authors' next paper.

Adaptive thermal comfort and building microclimate

Adaptive thermal comfort theory may be used to explain the comfort in a free-running building, since the relationship between indoor comfort temperature and outdoor monthly mean temperature for free-running buildings was found to be closely linear in Humphreys's field survey (Nicol & Humphreys, 2002). According to Humphreys's opinion, it is in principle possible to design and operate buildings that provide comfort in the free-running mode, at least within a range of prevailing mean outdoor temperatures from 10 to 30°C (Humphreys, Rijal, & Nicol, 2013). However, when talking about thermal comfort, a distinction is always made between indoor thermal comfort and outdoor thermal comfort. In this paper, the authors put forward the idea that thermal comfort should be considered at the building microclimate scale in terms of combining the indoor and outdoor thermal comfort to evaluate the thermal comfort in free-running buildings with diverse spaces during the summer, especially in the hot and humid climate area. This is based on adaptive thermal comfort theory.

Adaptive comfort is based on the concept that thermal comfort is highly influenced by personal preference and contextual factors that are commonly found in naturally ventilated buildings (Nicol & Humphreys, 2002). The fundamental assumption of the adaptive approach is expressed by the adaptive principle: "if a change occurs such as to produce discomfort, people react in ways which tend to restore their comfort". There are five basic types of adaptive actions: 1) regulating the rate of internal heat generation 2) regulating the rate of body heat loss 3) regulating the thermal environment 4) selecting a different thermal environment 5) modifying the body's physiological comfort conditions (Nicol et al., 2012).

One of the most important adaptive behaviours related to building components is the opening of windows and doors. Opening windows is one of the most favoured adaptive measure across countries (Mishra & Ramgopal, 2013). In a field survey conducted in Changsha, China, the opening of windows and doors was found to be the most frequently used adaptive action (Liu et al., 2012). The main goal of opening windows or doors is to obtain more air movement and fresh air. In this respect, a large opening in all the walls can provide the design solution for effective cross ventilation in the hot and humid climate areas, especially for free-running buildings (Givoni, 1994). Examples can be found in many vernacular buildings in tropic or sub-tropic climate areas such as Australia, India, Indonesia, Malaysia, Singapore, Thailand, Vietnam and China. If the windows or doors are big enough, the point at which the indoor space stops and the semi-outdoor or outdoor space begin will blur (figure 5.1). The indoor space can thus be changed to a semi-outdoor space.

Another important adaptive behaviour is movement. When people are free to choose their location, it helps if there is plenty of thermal variety, giving them the opportunity to choose the places they like (Humphreys, 1997). Occupants can change their location for different activities. Movement is possible between buildings, between rooms, around rooms, out of the sun and into the breeze, and so on (Nicol et al., 2012). Buildings with diverse spaces provide opportunities for movement. Indoor space, semi-outdoor space and outdoor space are the three typical kinds of space. These types of spaces are also emphasised in architectural spatial design. Atria, corridor, porch, patio and courtyard are commonly utilized elements to provide diversity in the types of space in the building. In hot and humid climates, occupants prefer to move from indoor spaces to semi-outdoor spaces. Occupants can expand their comfort from this adaption in two ways: physiologically as more air movement can influence the comfort sensation, and psychologically as people prefer an open environment in summer. The field survey about occupants' adaptive movement in the building is limited. Part of the reason is that in modern buildings the opportunities for movement on the part of occupants are restricted. If opportunities for movement are not available to the building occupants, only the indoor thermal comfort is considered, which does not reflect the true comfort situation, as the semi-outdoor and outdoor thermal comfort are also should be evaluated. The diversity in spaces and thermal environment in the building microclimate provides a range of choices for human's action which produces a different thermal environment.

According to Nicol et al. (2012), "The key to mastering the skill of producing comfortable, low-carbon building is to look at the 'whole system' when designing. The adaptive comfort approach helps us here because it works with many attributes of the system. The outside climate, the building's context, its form, services and occupants as well as the seasons and times of day are all part of this complex package of attributes that determine our comfort in a system". The building microclimate in a building is such a system and can be characterized as: dynamic and interactive, changing, customary and seasonally adjusted.

Evaluation of thermal comfort in the building microclimate using the adaptive approach

One of the main outcomes of the adaptive approach is the thermal comfort evaluation method based on field studies, in which the indoor thermal comfort temperature is shown to be a function of the outdoor temperature. The equation is:

$$T_n = A + BT_o$$

Where T_n is the neutral or comfort temperature (°C); T_o is the mean outdoor air temperature (°C); A, B are the constants. The constants A and B are different in different climate regions and cultural contexts. They can be confirmed by field survey in different regions. Some of the equations, especially applied to China for free-running buildings, are listed in table 5.1.

TABLE 5.1 Adaptive comfort equations

Location (source)	Equation
Humphreys (Humphreys & Nicol, 1998)	$T_n = 11.90 + 0.534T_o$
ASHRAE Standard 55-2010 (ANSI/ASHRAE, 2017)	$T_n = 17.80 + 0.31T_{ref}$
China (general) (Yang, 2003)	$T_n = 19.70 + 0.30T_o$
Shanghai, China (Ye et al., 2006)	$T_n = 15.12 + 0.42T_o$
Chongqing, China (Li, 2008)	$T_n = 16.28 + 0.39T_o$
Harbin, China (in summer) (Wang et al., 2010)	$T_n = 11.802 + 0.468T_o$

Here T_n is the neutral comfort temperature (°C); T_o is outdoor monthly mean temperature (°C); T_{ref} is the prevailing mean outdoor air temperature (°C) (for a time period between last 7 and 30 days before the day in question)

Another important issue relating to adaptive comfort is the influence of humidity and wind velocity. In free-running or naturally ventilated buildings, the influence of humidity and wind velocity on occupants' thermal comfort sensation in hot and humid climate regions is greater than in other climate regions and in conditioned buildings. The cooling effect of air movement depends on, not only air velocity, but also temperature, humidity and radiation balance, as well as on the activity (metabolic rate) and clothing of the individual (Szokolay, 2000). Studies done in different climates show occupants prefer greater air movement and comfort ranges can expand with the aid of air movement (Mishra & Ramgopal, 2013). In hot and humid climate areas, air movement can promote convective heat transfer from the skin and increase the evaporation of sweat. Occupants appreciate air movement, even when it is not necessary for cooling action (Zhang et al., 2007).

In order to approximate the potential cooling effect of an elevated air velocity to compensate for a room's high operative temperature, Nicol (2004) proposed the raise in comfort temperature caused by the air movement as:

$$\Delta T = 7 - \frac{50}{4 + 10V_a^{0.5}}$$

Where ΔT ($^{\circ}\text{C}$) is the raise in comfort temperature and V_a (m/s) is the air velocity and the equation is applicable when V_a consistently remains above 0.1m/s. This equation is also included in EN15251. Szokolay (Szokolay, 2000) proposed the function as follows, based on the analysis of other 11 equations adopted by other researches.

$$\Delta T = 6V_e - 1.6(V_e)^2$$

Where ΔT ($^{\circ}\text{C}$) is the cooling effect compensated for by the elevated air velocity, V_e is the effective velocity ($V_e = V - 0.2$ m/s); where V is the air velocity at the body surface); the equation is valid up to 2m/s (Szokolay, 2000). Su et al. (2009) derived two equations for the influence of wind velocity and relative humidity on thermal comfort in China based on other researcher's studies:

1) If the relative humidity exceeds 70%, the thermal temperature will ascend 0.4°C per 10% increase in relative humidity on the premise that the indoor air temperature exceeds 28°C .

2) The thermal temperature will decrease 0.55°C with a 0.15m/s increase of airflow velocity.

When indoor air temperature is over 28°C :

$$\Delta T = -4(\varphi - 70\%) + \frac{0.55V}{0.15}$$

When indoor air temperature is below 28°C :

$$\Delta T = \frac{0.55V}{0.15}$$

Where ΔT ($^{\circ}\text{C}$) is the cooling effect compensated for thermal neutral temperature by relative humidity and elevated air velocity, Φ is the relative humidity (if less than 70%, $\Phi = 70\%$) and V is the air velocity at the body surface. The equation is valid up to 0.8m/s. This equation will be adopted in the section 5.4.2.2 for the evaluation of thermal comfort in the vernacular house as it obtained from Chinese climate condition.

5.3 Methodology

Vernacular architecture, built by people whose design decisions were influenced by local climate and culture, has been gleaned through a long period of trial and error and the ingenuity of local builders who possess specific knowledge about their location, and thus are valuable in promoting the bioclimatic design approach to modern buildings (Zhai & Previtali, 2010). In many traditional buildings, bioclimatic design strategies are utilized to achieve an appropriate building microclimate for thermal comfort. In the present study, in order to investigate the building microclimate and evaluate the thermal comfort in a single building, a typical Chinese vernacular house, situated in Chongqing, in the hot and humid climate area of China, was studied. First, measurements were taken on site on two typical summer days. Air temperature and the relative humidity were measured at measured points distributed across various spaces. Wind velocity was also gauged in the key spaces. Thermal and CFD simulations were also performed because of the limited measurement equipment to predict the distribution of air temperature, relative humidity and wind velocity as well as to analyse the thermal comfort in the vernacular house in summer. The simulation results are validated with the field measurements.

5.3.1 The Chinese vernacular house

The house that formed the object of the study is located in Shuangjiang Town of Tongnan County, Chongqing China, located in the Sichuan Basin in the western part of the hot summer and cold winter climate zone (eastern longitude 105°17'–110°11' and northern latitude 28°10'–32°13'). Table 5.2 (National Meteorological Information Center of China Meteorological Administration & Department of Building Technology Tsinghua University, 2005) shows the monthly climate data in the typical meteorological year of Chongqing. In the typical meteorological year, the annual average temperature there is 18.4°C; the average temperature in the hottest month is 28.1°C and in the coldest month is 8.1°C; the highest temperature is 37.7°C in August and the lowest temperature is 2.8°C; the annual relative humidity is around 70%-80%. The average wind velocity in summer is 1.6 m/s and the prevailing wind comes from the north-west.

TABLE 5.2 Monthly climate data of Chongqing in the typical meteorological year

Month	1	2	3	4	5	6	7	8	9	10	11	12
Average air temperature (°C)	8.1	10.3	13.7	18.7	23.0	25.2	28.1	27.6	24.1	18.4	14.6	9.2
Max air temperature (°C)	13.6	19.5	25.1	29.7	34.9	35.4	36.6	37.7	34.5	27.9	23.1	15.2
Min air temperature (°C)	3.4	2.8	8.2	10.8	15.3	18.2	22.2	19.9	18.5	12.1	7.0	2.8
Average relative humidity (%)	85	82	77	81	74	81	77	76	81	83	85	86
Average wind velocity (m/s)	1.3	1.4	1.6	1.5	1.6	1.5	1.6	1.7	1.4	1.1	1.4	1.1

The summer here is extremely hot, humid and uncomfortable. A survey showed that 60–90% of the local population complained of sleeplessness on summer nights due to the sweltering heat and sultry weather. Air conditioning is used on a wide scale in the urban area. According to a survey carried out in 1997, average daily electricity consumption could rise to 20 kWh per household in Chongqing during a summer season (Fu, 2002).

The object of this study is Yang’s house, built in the Qing Dynasty and representing more than 120 years of history. Figure 5.2 shows the location and bird’s-eye view of the house. The building is well-preserved, except for minor building maintenance and repairs, and it completely retains the original architectural form and spatial distribution. In addition, its shape and structure are that of a typical Chinese vernacular building with quadrangle courtyards (the enclosed courtyard is surrounded by building groups or walls). The whole building covers an area of about 3500 m² with the maximum depth of 85 m and the maximum width of 53 m, and the building area is about 1768 m². There are 3 main courtyards, 10 patios and 51 rooms in different sizes. Most of the building has one floor and there are only a few attics. The spatial distribution and images of the house are shown in figure 5.3. The main construction is formed by the traditional timber-framed structure. The building is composed of lightweight walls, windows and doors. Primary construction materials are wood (for the main structure, enclosure structure, bedroom ground etc.), grey tiles (for roofs), stone material (for enclosing walls and ground floor) and brick (for enclosing walls).



FIG. 5.2 Location and bird's-eye view of "Yang's house" in Shuangjiang town of Tongnan, Chongqing

5.3.2 Field measurements

A period of continuous measurements took place in 2012, from 12:00 on August 28th to 12:00 on August 30th. Measurements were taken of the temperature, relative humidity, and the wind velocity in key positions at the measured points. The position of the measured points for temperature and relative humidity is shown in figure 5.3. Use was made of an automatic temperature logger and temperature and humidity logger, which recorded data every five minutes. Temperature accuracy was 0.2°C; the accuracy of relative humidity was 5%. The equipment was placed above the ground at a height of 1.2 m at the measured points both indoors and outdoors. The position of the measured wind velocity on August 28th was in the middle of the multifunctional room (m-room). The wind velocity was recorded every five minutes in the measured period. The position of the measured wind velocity in the afternoon of August 29th is shown in figure 5.3. The wind velocity was measured five minutes at every point and the average wind velocity was recorded. The accuracy of the readings of the manual anemometer was 5% reading add 0.05 m/s. Weather conditions on the test days of August 28th and 29th were partly cloudy with occasional rain at night, which is typical summer weather in the Chongqing area. Since it rained during the day on August 30th, the following analysis will focus on August 28th and 29th.

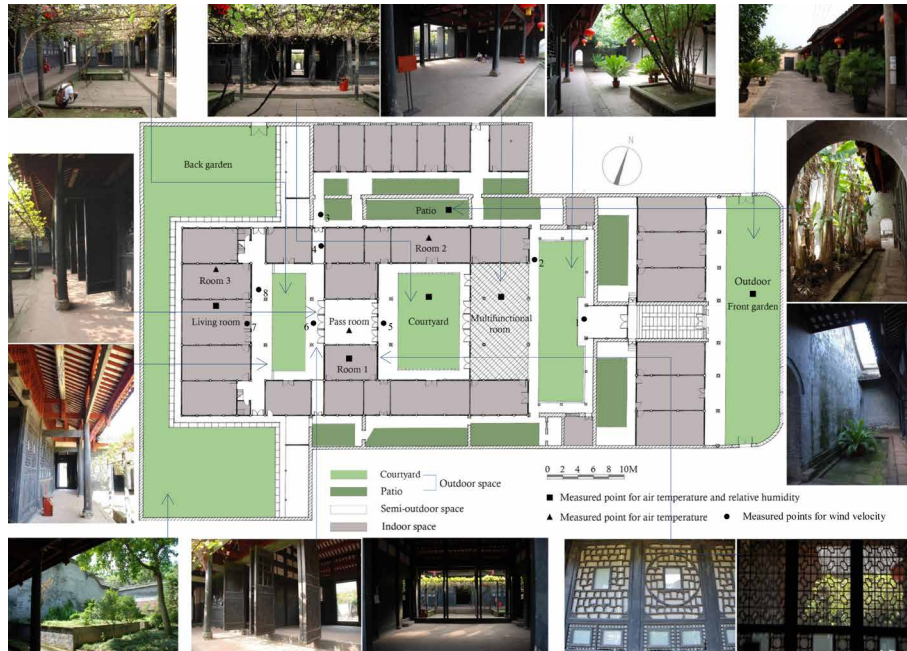


FIG. 5.3 The plan, measured points, spatial distribution and images of the vernacular house

5.3.3 Thermal and CFD simulation

Because of the limited number of measurement points, a thermal simulation was performed to obtain the temperature and humidity distribution in the building over a large time period and a CFD simulation was performed to predict the airflow distribution in the building.

Thermal simulation

The thermal simulation was performed with DesignBuilder(DB) software. DB is one of the most comprehensive user interfaces for the EnergyPlus dynamic thermal simulation engine. Figure 5.4(a) (b) shows the 3D model of the vernacular building in DB. Because of the limitation of the software, i.e. it cannot simulate the outside temperature, the courtyards and patios were modelled as atria. In the model, roof windows of the atria are constantly open and some shading was simulated as well, to simulate the presence of trees in the courtyards and patios (figure 5.4 (c)). This

model's simulation of the courtyards and patios will impact the accuracy of the thermal and CFD simulation, as the model's roof windows and shading is not exactly the same as the vegetation in the courtyards and patios. However, it is assumed that the accuracy is enough for the analysis in the present research which is comparing the measurements to the simulations and predicting the temperature over a large time period and in all the rooms.

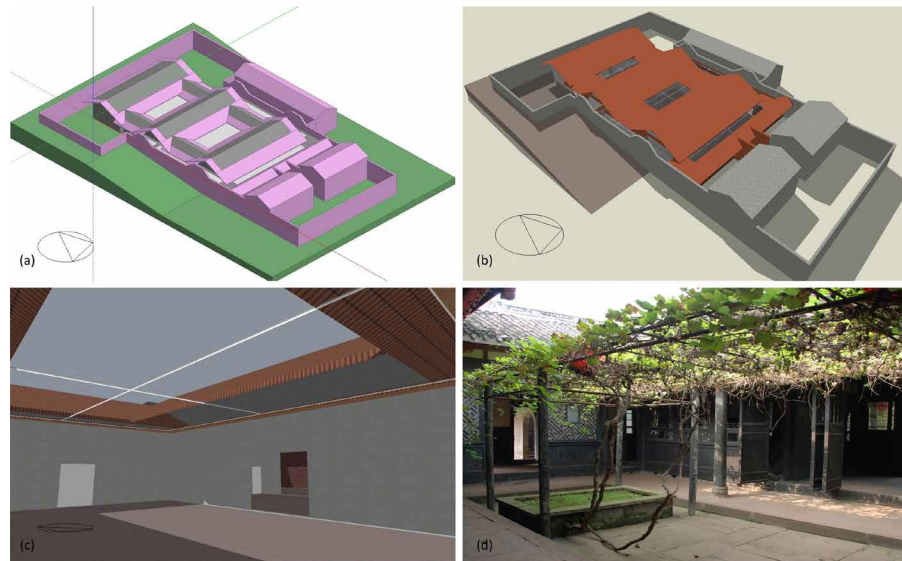


FIG. 5.4 The simulation model (top) The model of the studied vernacular house (bottom left) The rendered model (bottom right) The comparison of model and real courtyards

The entire building energy simulation was performed using the Chinese typical meteorological year weather (CTYW) data from Energyplus weather data sources. The hourly weather data in Chongqing, which is the nearest weather station to the measured subject, was utilized. The thermal simulation was performed during the whole summer time from June 1st to August 31st. Figure 5.5 shows the input weather data in the simulated period. Based on the weather data, the temperature was relative mild from June to the middle of July. The temperature changed quickly and was unstable in this period. From the middle of July to the first ten-days of August, the temperature was at a stable high level. These 20 to 25 days were the hottest days in summer. After that, the average temperature decreased and some days were relative warm. The mentioned summer climatic characteristics above are in agreement with the local summer climate and local occupants' experiences in summer. According to the utilized weather data, it was found that the solar radiation

in the summer in the studied area remained at a high level, especially in July and August. This is agreement with the fact that there is strong solar radiation in summer and that the maximum value is beyond 500MJ/m² and the total solar radiation in July and August accounts for 31% of yearly radiation (National Meteorological Information Center of China Meteorological Administration & Department of Building Technology Tsinghua University, 2005).

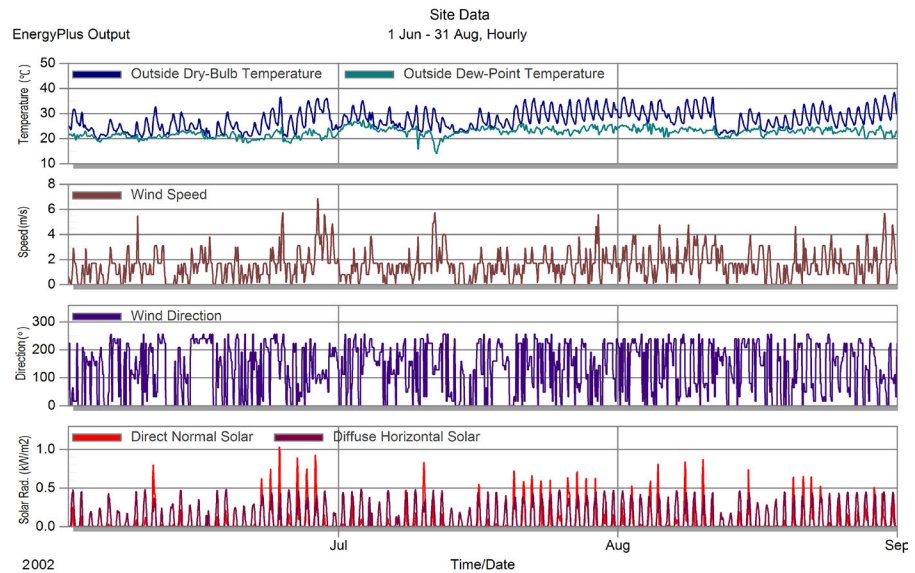


FIG. 5.5 The used weather data for the thermal simulation

The characteristics of the simulated house and the characteristics of building components are shown in table 5.3. The building performed as a free-running building with natural ventilation without any heating or cooling, corresponding to the real situation of the building. Thus, the windows on the outside walls were assumed 70% opened, internal windows were assumed 60% opened and roof windows were completely opened; all of the doors were assumed 90% opened in the simulation period. The infiltration was switched off since infiltration heat flows through the cracks are only a very small part of summertime air flow with the windows of the outside wall 70% opened. For validation, the simulation results will be compared with the field measurements taken on the test day.

TABLE 5.3 Characteristics of the simulated house and the building components

Characteristics /component	Description
Location	Chongqing
Running model	Free-running
Activity	Without occupant and equipment
Natural ventilation	Natural ventilation-no heating/cooling, calculated, constant
Construction	
External wall	Wood, dry, 20mm, U-Value=3.476(w/m ² -k)
Internal wall	Wood, dry, 20mm, U-Value=3.476(w/m ² -k)
Internal floor	Stone, sand stone, 500mm, U-Value=1.71(w/m ² -k)
Roof	Tile, 40mm; air gap, 20mm; woods, 50mm; U-Value=1.507(w/m ² -k)
Glazing	
Outdoor	Uninsulated, clear 6mm, U-Value=5.778(w/m ² -k), 70% opened
Indoor	Uninsulated, clear 6mm, U-Value=5.778(w/m ² -k), 60% opened
Roof window	Uninsulated, clear 6mm, U-Value=5.778(w/m ² -k), 100% opened, with shading

CFD simulation

For air velocity assessment, a validated CFD model is necessary since other methods are not able to provide detailed information on the performance of a natural ventilation strategy (Chen, 2009). In the present study, the CFD code from the DB software was used. The numerical method used by DBCFD is known as the primitive variable method, and comprises the solution of a set of equations that describe the conservation of heat, mass and momentum. The equation set includes the three velocity component momentum equations (known as the Navier-Stokes equations), the temperature equation and where the k-ε turbulence model is used, equations for turbulence kinetic energy and the dissipation rate of turbulence kinetic energy. The equations comprise a set of coupled non-linear second-order partial differential equations having the following general form, in which Φ represents the dependent variables:

$$\frac{\partial}{\partial t}(\rho\phi) + \text{div}(\rho u\phi) = \text{div}(\Gamma \text{grad}\phi) + S$$

Where the $\frac{\partial}{\partial t}(\rho\phi)$ term is the rate of change, the $\text{div}(\rho u\phi)$ term is convection, the $\text{div}(\Gamma \text{grad}\phi)$ term is diffusion and S is source term.

The boundary conditions for DB's CFD simulations, such as the input weather data, building's constructional components, opening sizes and operation schedule were established from previously calculated values using the thermal modelling software EnergyPlus, which was also run from within the DB environment. Thus, an accurately built model and correct input parameters were ensured to give accurate CFD results. In DB CFD package, there are two general approaches to natural ventilation modelling: scheduled and calculated natural ventilation. In this case, the calculated natural ventilation model was used where the ventilation rates between the zones are calculated using wind and buoyancy-driven pressure, opening size and operation. DB uses the Energyplus Airflow Network method to calculate air flow rates which can be described as following equation:

$$Q = C_d A \sqrt{\frac{2\Delta P}{\rho}}$$

Where Q is the air flow rate (m^3/s); C_d is the opening's discharge coefficient; A is the opening's area (m^2); ΔP is the pressure difference across the opening or crack (Pa); ρ is the density of air (kg/m^3). The default value of opening's discharge coefficient 0.65 was utilized in this case. For wind-driven ventilation situation, the pressure on any point on the surface of the building façade can be represented by:

$$P = 0.5\rho C_p V^2$$

Where P is the surface pressure due to wind (Pa); ρ is the density of air (kg/m^3); C_p is the wind pressure coefficient; V is the wind velocity (m/s). The wind pressure coefficient C_p is a function of wind direction, position on the building surface and side exposure. DB provides default wind pressure coefficients suitable for use in basic design calculations for buildings having no more than three stories. In this case, the building is only one storey, thus the default settings of wind pressure coefficients were utilized.

The grid used by DBCFD is a non-uniform rectilinear Cartesian grid, which means that the grid lines are parallel with the major axes and that the spacing between the grid lines enables non-uniformity. In this case, the grid spacing was adopted that is generated with 0.2 m with a 0.025 m grid line merge tolerance. The details related to the CFD simulation set up in the present case are summarized in table 5.4.

TABLE 5.4 Summary of CFD cell setting and time steps

Total cells	530469
Cell size	0.2 m
Max aspect ratio	6.045
Iterations	15000
False time step	0.10

5.4 Results and analysis

5.4.1 The results of the field measurement

Temperature and relative humidity

Figure 5.6 shows the air temperature and relative humidity of the measured vernacular house in the period from 12:00 on August 28th to 24:00 on August 29th 2012. The analysis will mainly focus on August 29th, as measurements were taken throughout the entire day. The positions of the test points were shown in figure 5.3.

On August 29th, the lowest measured outdoor temperature was 24.3°C. The outdoor temperature then started to rise at 7:00, peaked at 36.6°C at 14:00, after which it went back down.

Figure 5.6 (a) shows the comparison of the outdoor air temperature and indoor air temperature (room1, room2, room3 and living room). From 00:00 to 07:00 on August 29th, the measured indoor air temperatures remained at almost the same level as the outdoor temperature. As can be seen, the difference was small. The indoor air temperatures then began rising at 07:00 (with a small time delay in room1 and room3). The temperature in room1, room3 and the living room peaked at 31.0°C-31.3°C at around 16:40. The temperature in room2 reached a peak of 32.5°C at 15:00. An obvious time delay was seen in the max temperature between the air temperature outdoors and indoors. The results showed that an indoor air temperature was around five degree lower than the outdoor air temperature during

the day and a time delay of the peak temperature of around two and half hours. At night, the heat in the building quickly dissipated and the indoor temperature then approached the outdoor temperature, resulting in thermal comfort.

Figure 5.6 (b) shows the comparison of the outdoor, courtyard and patio air temperature and semi-outdoor air temperature (pass room and multifunctional room). From 00:00 to 07:00 on August 29th, all of the semi-outdoor air temperatures remained at almost the same level as the outdoor temperature. As can be seen, the difference was small. The semi-outdoor air temperatures then began rising at 07:00. The temperature in the courtyard reached a peak of 35.3°C at 14:30; the temperature in the multifunctional room peaked at 33.0°C at 15:00; in the pass room the temperature peaked at 32.6°C at 15:00; and in the patio at 31.5°C at 15:00. During the day, the courtyard air temperature was one degree lower than the outdoor temperature due to the vegetation in the courtyard. The semi-outdoor air temperature was some 3-4°C lower than the outdoor temperature and the time delay of the peak temperature was about 1 hour. The patio temperature was five degree lower than the outdoor temperature, as the patio receives no direct solar radiation due to the lush vegetation and narrow opening.

In Figure 5.6 (c), the outdoor and patio air temperature, the semi-outdoor air temperature (multifunctional room) and the typical indoor air temperature (living room) are compared. From 00:00 to 07:00 on August 29th, both the semi-outdoor air temperatures and the indoor air temperature remained at almost the same level as the outdoor temperature. At 07:00, these temperatures reached their lowest point around 24.3°C. The semi-outdoor peak temperature was higher than the indoor temperature, but much lower than the outdoor temperature. The patio temperature in particular was lower than the outdoor temperature, with a maximum difference of around 5°C which was almost equal to the indoor temperature.

Figure 5.6 (d) shows the distribution of the air temperature in the different spaces at different times. The graphs clearly indicate that there is a remarkable difference in air temperature in the different spaces of the building during the day-time. It was found that as the outside air temperature rises, the temperature difference also increases. In other words, the outdoor temperature was higher than the semi-outdoor temperature and the semi-outdoor temperature was higher than the indoor temperature. In contrast, at night, the air temperature returned to the same level in the different spaces.

In general, the relative humidity followed the air temperature during the day. At night, humidity levels mostly exceeded 70%. Indoor relative humidity was higher than semi-outdoor relative humidity, which in turn was higher than the outdoor levels measured, whether at night or in the daytime; see figure 5.6 (e).

Air velocity

Figure 5.7 shows the air velocity measurements taken every five minutes in the multifunctional room of the vernacular house from 14:00 to 17:00 on August 28th. The air velocity was between 0-1.8m/s and can be characterized as an unstable gust with fluctuations. The average air velocity was 0.74m/s, which is higher than the average air velocity of 0.26 m/s measured outdoors.

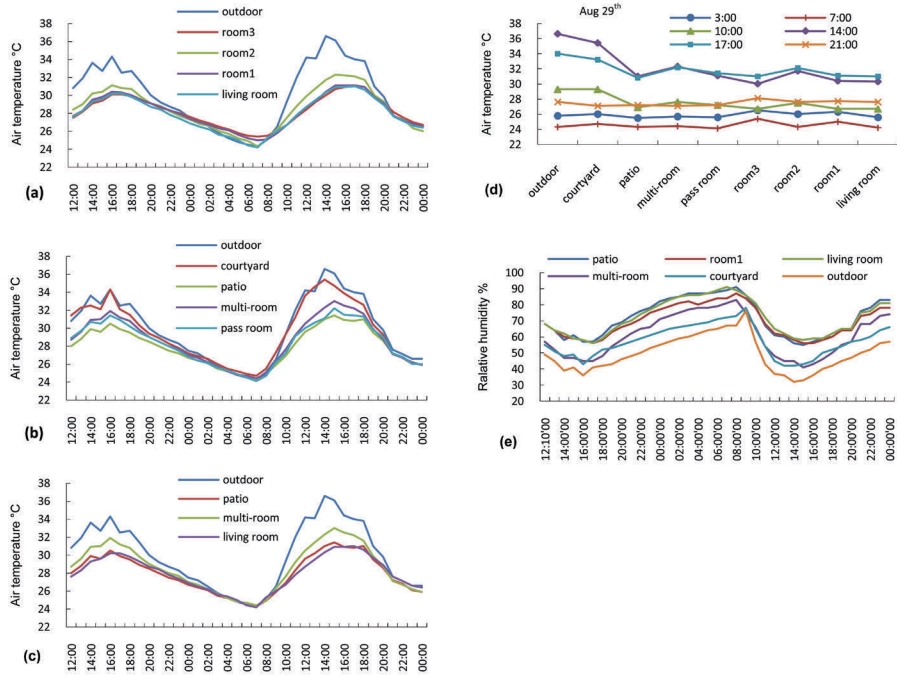


FIG. 5.6 Measured hourly results of temperature and relative humidity in the vernacular house on 28/29 Aug 2012

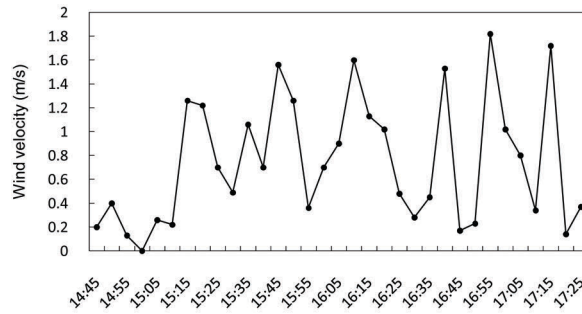


FIG. 5.7 Measured results of wind velocity on Aug 28th

5.4.2 Simulation results

5.4.2.1 Thermal simulation results

Comparisons with measurements

The hourly temperatures of the house during the summer time were obtained from the simulation. In figure 5.8, the simulated outdoor air temperature and air temperature in the different spaces, from 12:00 on August 28th to 24:00 on August 29th, is compared with the field-measurements. Figure 5.9 shows the T_m/T_s (T_m is the measured air temperature and T_s is the simulated air temperature) of all the measured points. The simulated results were found to fit well with the test results except for the time period after 18:00 on August 29th. The air temperature changes from the simulated results were matched with the measured results. On August 29th, differences between the measured temperature trends and the simulated trends were only seen after 18:00. These were caused by the accuracy of the weather data used in DB. Generally, the simulated temperature was higher than the measured temperature, especially at night. Nonetheless, all of the test data fell within a 15% range of the simulated data and the average difference was within 5% (figure 5.9). Hence, the same conclusion can be drawn from the simulations as from the field measurements: the temperature difference in the different spaces and rooms can be measured and simulated for this building using dynamic hourly temperature calculations.

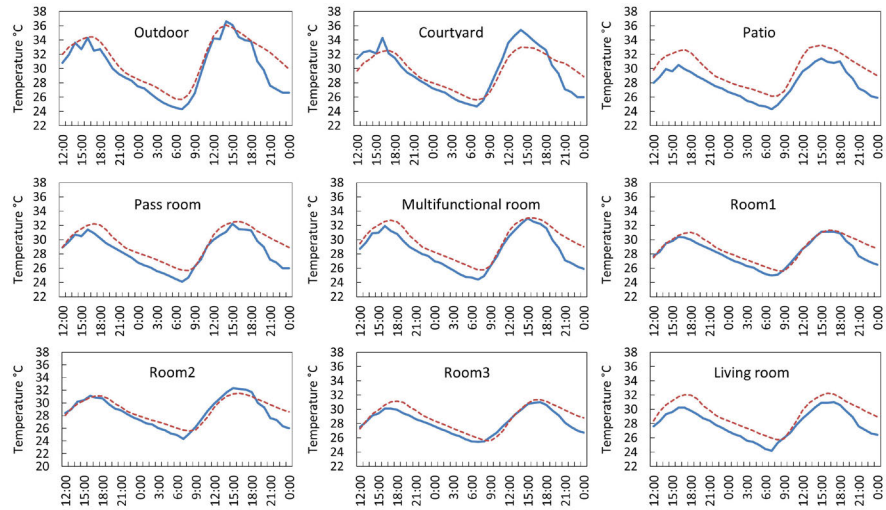


FIG. 5.8 Comparison of simulated and measured results in temperature on 28/29 Aug 2012

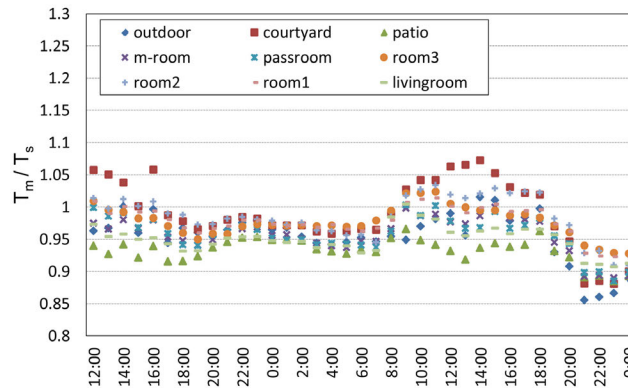


FIG. 5.9 The T_m/T_s of measured points on 28/29 Aug 2012 (T_m is the measured temperature and T_s is the simulated temperature)

Comfort

The adaptive comfort model is used to evaluate the thermal comfort in this vernacular house. For the present location, the proposed relationship between thermal comfort temperature and monthly mean outdoor temperature in the Chongqing area is:

$$T_n = 16.28 + 0.39T_o$$

Where T_n is the comfort temperature ($^{\circ}\text{C}$) and T_o is the monthly mean outdoor temperature ($^{\circ}\text{C}$); the range is 5.0°C – 30.0°C (Li, 2008). According to this equation, the comfort temperatures in June, July and August are: 25.7°C , 26.6°C and 26.9°C . According to ASHRAE Standard 55, a comfort zone band of $\pm 2.5^{\circ}\text{C}$ corresponds with 90% acceptability, and $\pm 3.5^{\circ}\text{C}$ corresponds with 80% acceptability. So, the comfort zone, which in this case corresponds to 90% acceptability, ranges from 23.2°C – 28.2°C in June, 24.1°C – 29.1°C in July to 24.3°C – 29.3°C in August. Figure 5.10 shows the simulated results of the operative temperature in the living room, which had the lowest measured temperature during the day, in June–August and the comfort temperature zone based on the local climate in this period. The comfort temperature zone based on ASHRAE Standard 55–2010 is also shown in figure 5.10 as the reference to the equation for comfort temperature calculation used in Chongqing area. According to the local summer climatic features analysis in section 5.3.3, in the relative mild days in terms from June to the middle of July, the operative temperature was lower than the comfort upper temperature limit in most of the days. The building can provide a comfortable thermal environment for the occupants without mechanical cooling. In the hottest days, during the middle of July to the first ten–days of August, almost all of the operative temperatures in the daytime exceed the comfort upper temperature limit. The comfort thermal environment cannot be achieved in the building with the free–running model, even if the building has a very good passive cooling design. In the relative warm days, during the middle and last ten days, the uncomfortable time was limited and the thermal environment in the building could be accepted most of the time. Generally, during the entire summer, it was found that a comfortable temperature could be achieved most of the time in the building. However, around 1/3 of the daytime, the temperature exceeded the upper temperature limit of the comfort zone. In other words, in summer time, a comfortable indoor thermal environment could be achieved in the vernacular house around 2/3 of the daytime, and the operative temperature was lower than the upper limit comfort temperature at night. However, as shown in section 5.2.2, an increased air movement can increase the comfortable temperature. In the following section, the air velocity for thermal comfort in the different spaces will be analysed.

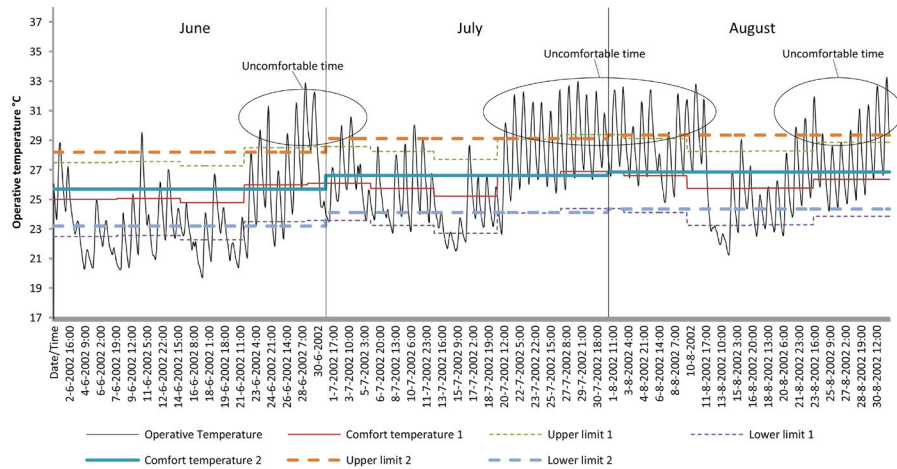


FIG. 5.10 The simulated operative temperature of living room and comfort temperature zone for 90% acceptability (1-Based on ASHRAE Standard 55-2010, 2-Based on the equation for Chongqing area)

5.4.2.2 CFD simulation results

As mentioned before, the boundary conditions of the CFD simulation in DB derive from the thermal simulation. This has been done in DB in order to achieve more accurate results in CFD. The validation of the thermal simulations compared with the field measurements was described in the previous section. One way to validate the CFD is to compare the results with the measured wind velocity. Figure 5.11 (a) shows the simulated wind velocity distribution in the whole building at 14:00 on the 29th of August and the measured points 1-8 for validation. Table 5.5 shows the measured and simulated wind velocity at the 8 points which were distributed in the different position of the vernacular house. Figure 5.12(a) shows the comparison of measured and simulated wind velocity and figure 5.12 (b) shows the ratio of measured and simulated wind velocity (V_m/V_s). It was found that point 1, 2, 4 and 7 displayed a relatively large difference between the measured and simulated results and the measured and simulated wind velocity at point 3, 5, 6 and 8 were matched well. General say, the trend of the measured and simulated wind velocity distribution matches well. It may therefore be assumed that the calculated wind velocities in other areas of the vernacular house are accurate enough to predict the trend.

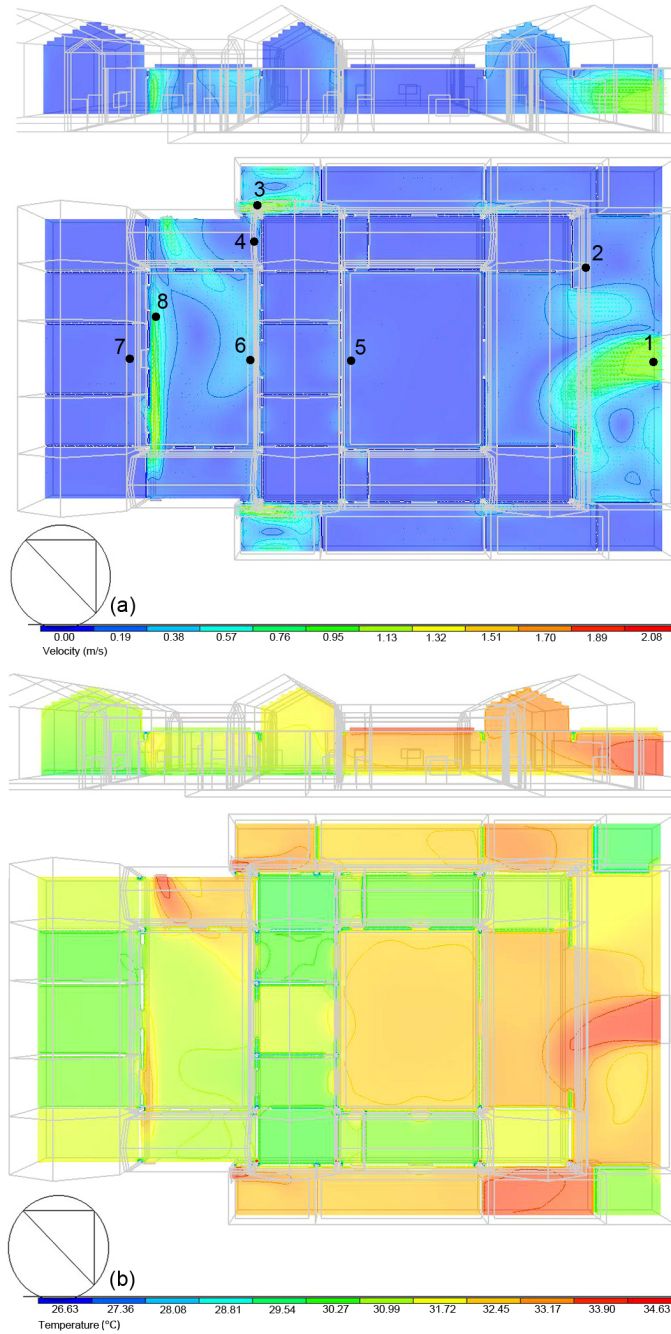


FIG. 5.11 The wind and temperature distribution at 14:00 Aug 29th (a) Wind distribution (b) Temperature distribution

TABLE 5.5 The measured and simulated wind velocity at different position of the vernacular house

Measured points	1	2	3	4	5	6	7	8
Measured wind velocity (m/s)	0.60	0.35	0.97	0.48	0.28	0.53	0.05	0.80
Simulated wind velocity (m/s)	0.95	0.25	0.95	0.30	0.25	0.57	0.20	0.80

The simulated wind velocity showed a clear difference in wind velocity in the various spaces in the building. The indoor wind velocity is low, below 0.2m/s. This is due to the fact that the window does not easily allow the passage of wind. The wind velocity in the centred courtyard and in some of the patios without openings was low that almost kept the same speed as the indoor wind velocity, as there was no opening for cross ventilation and neither the height nor the temperature difference between the bottom and top of the courtyard and patio was large enough for stack ventilation. The wind velocity in the courtyards and in some of the patios with openings was high between 0.6-1.1 m/s. In the semi-outdoor spaces, a wind velocity of 0.6m/s can be obtained in some areas of the multifunctional room. The wind velocity in the pass room was around 0.3m/s, which is not remarkably higher than the indoor wind speed. In the indoor spaces, there is no clear difference in vertical direction. However, in the courtyards and patios with openings, the wind velocity at the bottom was higher than at the top.

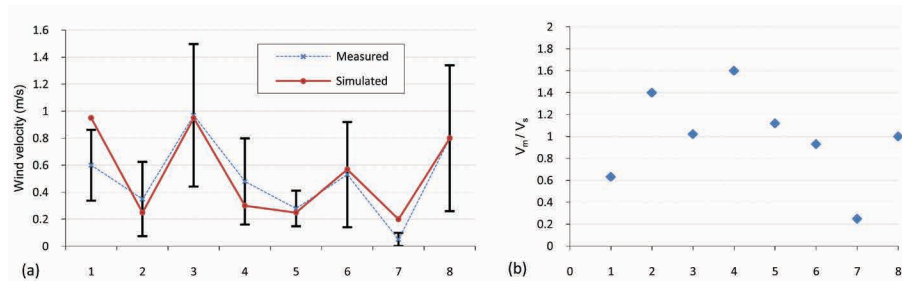


FIG. 5.12 (a) Comparison of measured and simulated wind velocity in different position (b) The ratio of measured and simulated wind velocity (V_m is the measured and V_s is the simulated wind velocity)

Combining the equation for thermal comfort calculation to Chongqing area and the equation for thermal comfort, taking into account relative humidity and wind velocity which mentioned in section 5.2.2, the equations for thermal comfort calculation here can be:

When indoor air temperature is over 28°C:

$$T_n = 16.28 + 0.39T_o - 4(\phi - 70\%) + \frac{0.55V}{0.15}$$

When indoor air temperature is below 28°C:

$$T_n = 16.28 + 0.39T_o + \frac{0.55V}{0.15}$$

Where T_n is the comfort temperature(°C), T_o is the monthly average of outdoor air temperature(°C), ϕ is the relative humidity (%) (if less than 70%, $\phi = 70\%$) and v is the wind velocity(m/s). This shows that wind and humidity impact on thermal comfort to a major extent.

At the time of simulation, relative humidity was lower than 70%, and the temperature was higher than 28°C. The comfort temperature at the points of the semi-outdoor and outdoor spaces can be calculated taking wind velocity into account (table 5.6). This shows that the occupants will feel more comfortable with 90% accept ability if they remain at points2, 3, 6, 7, 8 and with 80% acceptability if they remain at points 1-8. During daytime, occupants could move to semi-outdoor or outdoor spaces to perform their activities.

TABLE 5.6 The influence of wind velocity for adaptive thermal comfort at point 1-8

Location (points)	1	2	3	4	5	6	7	8
Simulated wind velocity (m/s)	0.95	0.25	0.95	0.30	0.25	0.57	0.20	0.80
Simulated air temperature (°C)	33.90	31.00	32.00	31.00	31.00	30.10	29.00	30.10
ΔT (°C) (Raise in comfort temperature)	3.48	0.92	3.48	1.10	0.92	2.09	0.73	2.94
T_n (°C) Comfort temperature	30.52	27.96	30.52	28.14	27.96	29.13	27.77	29.98
Upper limit temperature for 90% acceptability (°C)	33.02	30.46	33.02	30.64	30.46	31.63	30.27	32.48
Upper limit temperature for 80% acceptability (°C)	34.02	31.46	34.02	31.64	31.46	32.63	31.27	33.48

Figure 5.11 (b) shows the air temperature distribution according to the CFD simulation. It again shows that different temperatures occur in the indoor space, semi-outdoor space and outdoor space.

5.5 Conclusion

In this paper the authors have clarified the definition of building microclimate in free-running buildings. It is a type of microclimate, involving the indoor space as well as the spaces around the indoor spaces (semi-outdoor space and outdoor space) of one particular building. It is the extension of the indoor climate belonging to one single building. The spatial and the thermo-physical properties of the building microclimate were examined.

Building microclimate can help to create comfortable conditions for the occupants in summer, especially in the hot and humid climate areas. The essence of architectural bioclimatic design is to understand the local climate and utilize appropriate design strategies for building form generation and material selection, in order to create or modify the building microclimate required for a comfortable living environment. The adaptive thermal comfort model is suitable to evaluate the summer thermal comfort in the building microclimate, as its core assumption is that “if a change occurs such as to produce discomfort, people react in ways which tend to restore their comfort” (Nicol, 2002) and building microclimate provides this opportunities by taking all spaces (indoor, semi-outdoor and outdoor) of a single building into account.

A case study was conducted in a Chinese traditional vernacular house with quadrangle courtyards in the hot and humid climate area of China. The aim was to determine the summer building microclimate in the building and to assess its function with respect to thermal comfort based on the adaptive comfort approach.

The field measurements show that the present Chinese vernacular house has its own independent building microclimate in summer, which is in accordance with the main character of microclimate in terms of different distributions of solar gain, air temperature and wind velocity in different spaces. Firstly, even at night, the air temperatures in different spaces close to the outdoor temperature, with only slight differences between the different spaces. However, during the daytime a remarkable temperature difference developed between the spaces, with the maximum temperature varying from 31°C to 35°C. Secondly, the relative humidity differed in the various spaces. The relative humidity was higher at night than during daytime and the indoor humidity was higher than outdoors, both day and night. Thirdly, the wind velocity differed strikingly in the building especially during the daytime. The wind velocity was low in the indoor spaces, but rose considerably in some of the courtyards and patios.

The simulation results of the vernacular house could be matched well with the field measurements, hence have sufficient accuracy for the research objective. The building microclimate and thermal comfort can be predicted by simulation. According to the simulation, at night, a comfortable temperature could be obtained throughout most of the summer time while in the daytime the operative temperature was higher than comfortable temperature for one-third of the summer period when only looking at the operative temperature. Wind velocity in the semi-outdoor and outdoor spaces could improve the thermal comfort significantly. The thermal comfort environment would thus not only change in time but also in space.

It is possible to create comfortable conditions when not only the indoor climate is taken into account but the whole building microclimate, as the example of the Chinese traditional vernacular house shows. Obtaining an appropriate organisation of spaces in terms of outdoor space, semi-outdoor space and indoor space for solar control and natural ventilation was the main bioclimatic design strategy for thermal comfort in the vernacular house studied for this research. Utilising suitable material and vegetation also contributed to the good building microclimate. Based on the appropriate bioclimatic design, the microclimate in the building could be modified for more comfortable living environment. This yielded comfortable temperatures throughout most of the summer, especially at night and provided enough air flow to promote thermal comfort during the day time. Finally, different spaces were available to the occupants enabling them to adapt to the thermal conditions.

New buildings can be made more comfortable when taking the combination of adaptive thermal comfort and building microclimate into account. Inspiration can be drawn from this study summer microclimate in a Chinese vernacular house for a modern building's bioclimatic design. Creating an appropriate building microclimate in a building is important for the thermal comfort in summer in a hot and humid climate zone. A key issue in this respect is the fact that building form generation significantly influences the microclimate in a building. Therefore, in architectural design, appropriate building form and space are not only important in terms of aesthetics, function and landscape, but also in terms of building performance, and, especially thermal performance in summer. Building performance simulation can help the bioclimatic design to predict and achieve a good building microclimate.

The present study, however, is not without limitations. The field data were collected for a period of two days only and the wind velocity measurements demonstrate shortcomings due to the limited equipment; the climate data used for thermal simulation was based on the year 2002 and the distance the nearest weather station is not so close; the house studied had a large building volume, and it is unclear whether the building microclimate features discussed above might apply equally in

a small-volume building. Additional research is required in the future to investigate these problems. Further work is to investigate the building microclimate in a new modern house with diverse spaces and use the bioclimatic design principles to create a comfortable building microclimate in design practice. A Chinese rural house is planned as the case for an example of a free-running building.

Acknowledgments

The authors gratefully acknowledge professor Tang Mingfang and Zhou Tiejun from Chongqing University for the help of the field measurements.

References

- A.L. Martins, T., Adolphe, L., & E.G. Bastos, L. (2014). From solar constraints to urban design opportunities: Optimization of built form typologies in a Brazilian tropical city. *Energy and Buildings*, 76, 43-56. doi: 10.1016/j.enbuild.2014.02.056
- Al-Sallal, K. A., & Al-Rais, L. (2012). Outdoor airflow analysis and potential for passive cooling in the modern urban context of Dubai. [Article]. *Renewable Energy*, 38(1), 40-49. doi: 10.1016/j.renene.2011.06.046
- Andreou, E. (2013). Thermal comfort in outdoor spaces and urban canyon microclimate. *Renewable Energy*, 55, 182-188. doi: 10.1016/j.renene.2012.12.040
- Andreou, E. (2014). The effect of urban layout, street geometry and orientation on shading conditions in urban canyons in the Mediterranean. *Renewable Energy*, 63, 587-596. doi: 10.1016/j.renene.2013.09.051
- ASHRAE. (2010). ASHRAE standard 55-2010 Thermal environmental conditions for human occupancy. GA: ASHRAE Atlanta.
- Berkovic, S., Yezioro, A., & Bitan, A. (2012). Study of thermal comfort in courtyards in a hot arid climate. *Solar Energy*, 86(5), 1173-1186. doi: 10.1016/j.solener.2012.01.010
- Chen, Q. (2009). Ventilation performance prediction for buildings: A method overview and recent applications. *Building and Environment*, 44(4), 848-858. doi: 10.1016/j.buildenv.2008.05.025
- China, N. B. o. S. o. (2012). Annual report (Publication no. <http://data.stats.gov.cn/english/easyquery.htm?cn=E0103>). Available from National Bureau of Statistics of China National database, from National Bureau of Statistics of China
- Chun, C., Kwok, A., & Tamura, A. (2004). Thermal comfort in transitional spaces—basic concepts: literature review and trial measurement. *Building and Environment*, 39(10), 1187-1192. doi: 10.1016/j.buildenv.2004.02.003
- Dimoudi, A., Kantzioura, A., Zoras, S., Pallas, C., & Kosmopoulos, P. (2013). Investigation of urban microclimate parameters in an urban center. *Energy and Buildings*, 64, 1-9. doi: 10.1016/j.enbuild.2013.04.014
- Du, X., Bokel, R., & van den Dobbelssteen, A. (2014). Building microclimate and summer thermal comfort in free-running buildings with diverse spaces: A Chinese vernacular house case. *Building and Environment*, 82, 215-227. doi: 10.1016/j.buildenv.2014.08.022
- EN15251. (2007). Indoor environmental input parameters for design and assessment of energy performance of buildings addressing indoor air quality, thermal environment, lighting and acoustics. Brussels: European committee for standardisation.
- Fazia Ali-Toudert, Moussadek Djenane, Rafik Bensalem, & Mayer, H. (2005). Outdoor thermal comfort in the old desert city of Beni-Isguen Algeria. *climate research*, 28, 243-256.

- Fu, X. (2002). *Building energy saving technology in hot summer and cold winter region*. Beijing: China Architecture and Building Press.
- Gaitani, N., Mihalakakou, G., & Santamouris, M. (2007). On the use of bioclimatic architecture principles in order to improve thermal comfort conditions in outdoor spaces. [Article]. *Building and Environment*, 42(1), 317-324. doi: 10.1016/j.buildenv.2005.08.018
- Gaitani, N., Spanou, A., Saliari, M., Synnefa, A., Vassilakopoulou, K., Papadopoulou, K., . . . Lagoudaki, A. (2011). Improving the microclimate in urban areas: a case study in the centre of Athens. *Building Services Engineering Research and Technology*, 32(1), 53-71. doi: 10.1177/0143624410394518
- GB50176-93. (1993). *Thermal Design Code for Civil Building*. Beijing: China Planning Press.
- Geetha, N. B., & Velraj, R. (2012). Passive cooling methods for energy efficient buildings with and without thermal energy storage - A review. [Review]. *Energy Education Science and Technology Part a-Energy Science and Research*, 29(2), 913-946.
- Giannopoulou, K., Santamouris, M., Livada, I., Georgakis, C., & Caouris, Y. (2010). The Impact of Canyon Geometry on Intra Urban and Urban: Suburban Night Temperature Differences Under Warm Weather Conditions. *Pure and Applied Geophysics*, 167(11), 1433-1449. doi: 10.1007/s00024-010-0099-8
- Givoni, B. (1994). *Passive and low energy cooling of buildings*. New York: Van Nostrand Reinhold
- Gulyás, Á., Unger, J., & Matzarakis, A. (2006). Assessment of the microclimatic and human comfort conditions in a complex urban environment: Modelling and measurements. *Building and Environment*, 41(12), 1713-1722. doi: 10.1016/j.buildenv.2005.07.001
- He, J., & Hoyano, A. (2010). Measurement and evaluation of the summer microclimate in the semi-enclosed space under a membrane structure. [Article]. *Building and Environment*, 45(1), 230-242. doi: 10.1016/j.buildenv.2009.06.006
- Heidari, S. (2000). *Thermal comfort in Iranian courtyard housing University of Sheffield Unpublished Ph.D. thesis*.
- Hu, X. (2008). Boundaries and openings: spatial strategies in the Chinese dwelling. *Journal of Housing and the Built Environment*, 23(4), 353-366. doi: 10.1007/s10901-008-9123-z
- Humphreys, M. A. (1997). An adaptive approach to thermal comfort criteria. In D. Clements Croome (Ed.), *Naturally Ventilated Buildings: Building for the Senses, the Economy and Society*. London E and FN Spon.
- Humphreys, M. A., & Nicol, J. F. (1998). Understanding the adaptive approach to thermal comfort ASHRAE Transactions, 104(1), 991-1004.
- Humphreys, M. A., Rijal, H. B., & Nicol, J. F. (2013). Updating the adaptive relation between climate and comfort indoors; new insights and an extended database. *Building and Environment*, 63, 40-55. doi: 10.1016/j.buildenv.2013.01.024
- Hwang, R.-L., & Lin, T.-P. (2007). Thermal Comfort Requirements for Occupants of Semi-Outdoor and Outdoor Environments in Hot-Humid Regions. *Architectural Science Review*, 50(4), 357-364. doi: 10.3763/asre.2007.5043
- Li, Y. (2008). *The study of the ventilation period and the effectiveness of control in residential building of Chongqing*. master, Chongqing University, Chongqing.
- Liang, J., Li, B., Wu, Y., & Yao, R. (2007). An investigation of the existing situation and trends in building energy efficiency management in China. *Energy and Buildings*, 39(10), 1098-1106. doi: 10.1016/j.enbuild.2006.12.002
- Lin, T.-P., de Dear, R., & Hwang, R.-L. (2011). Effect of thermal adaptation on seasonal outdoor thermal comfort. *International Journal of Climatology*, 31(2), 302-312. doi: 10.1002/joc.2120
- Liu, W., Zheng, Y., Deng, Q., & Yang, L. (2012). Human thermal adaptive behaviour in naturally ventilated offices for different outdoor air temperatures: A case study in Changsha China. *Building and Environment*, 50, 76-89. doi: 10.1016/j.buildenv.2011.10.014
- Meir, I., & Roaf, S. (2003). Between Scylla and Charibdis: In search of the sustainable design paradigm between vernacular and high-tech. Paper presented at the PLEA, Santiago, Chile.
- Merghani, A. (2004). Exploring thermal comfort and spatial diversity. In K. Steemers & M. A. Steane (Eds.), *Environmental diversity in architecture* (pp. 195-213). London and New York: Taylor and Francis Group.
- Mishra, A. K., & Ramgopal, M. (2013). Field studies on human thermal comfort — An overview. *Building and Environment*, 64, 94-106. doi: 10.1016/j.buildenv.2013.02.015
- Muhaisen, A. S., & Gadi, M. B. (2006). Effect of courtyard proportions on solar heat gain and energy requirement in the temperate climate of Rome. *Building and Environment*, 41(3), 245-253. doi: 10.1016/j.buildenv.2005.01.031

- National Meteorological Information Center of China Meteorological Administration, & Department of Building Technology Tsinghua University. (2005). Chinese meteorological dataset for built thermal environment. Beijing: China Architecture & Building Press.
- Niachou, K., Livada, I., & Santamouris, M. (2008). Experimental study of temperature and airflow distribution inside an urban street canyon during hot summer weather conditions. Part II: Airflow analysis. *Building and Environment*, 43(8), 1393-1403. doi: 10.1016/j.buildenv.2007.01.040
- Nicol, F. (2004). Adaptive thermal comfort standards in the hot-humid tropics. *Energy and Buildings*, 36(7), 628-637. doi: <http://dx.doi.org/10.1016/j.enbuild.2004.01.016>
- Nicol, F., Humphreys, M. A., & Roaf, S. (2012). *Adaptive thermal comfort: principles and practice* London and New York: Routledge.
- Nicol, J. F., & Humphreys, M. A. (2002). Adaptive thermal comfort and sustainable thermal standards for buildings. *Energy and Buildings*, 34(6), 563-572. doi: [http://dx.doi.org/10.1016/S0378-7788\(02\)00006-3](http://dx.doi.org/10.1016/S0378-7788(02)00006-3)
- Oke, T. R. (1987). *Boundary layer climates* (second ed.). New Fetter Lane, London: Routledge.
- Oliver, P. (1997). *Encyclopedia of Vernacular Architecture of the World*. New York: Cambridge University Press.
- Pitts, A., & Saleh, J. B. (2007). Potential for energy saving in building transition spaces. *Energy and Buildings*, 39(7), 815-822. doi: 10.1016/j.enbuild.2007.02.006
- Santamouris, M., & Asimakopoulos, D. (1996). *Passive cooling of buildings*. London: James and James
- Santamouris, M., Gaitani, N., Spanou, A., Saliari, M., Giannopoulou, K., Vasilakopoulou, K., & Kardomateas, T. (2012). Using cool paving materials to improve microclimate of urban areas – Design realization and results of the flisvos project. *Building and Environment*, 53, 128-136. doi: 10.1016/j.buildenv.2012.01.022
- Santamouris, M., Georgakis, C., & Niachou, A. (2008). On the estimation of wind speed in urban canyons for ventilation purposes—Part 2: Using of data driven techniques to calculate the more probable wind speed in urban canyons for low ambient wind speeds. *Building and Environment*, 43(8), 1411-1418. doi: 10.1016/j.buildenv.2007.01.042
- Santamouris, M., & Kolokotsa, D. (2013). Passive cooling dissipation techniques for buildings and other structures: The state of the art. [Review]. *Energy and Buildings*, 57, 74-94. doi: 10.1016/j.enbuild.2012.11.002
- Shashua-Bar, L., & Hoffman, M. E. (2003). Geometry and orientation aspects in passive cooling of canyon streets with trees. [Article]. *Energy and Buildings*, 35(1), 61-68. doi: 10.1016/s0378-7788(02)00080-4
- Shashua-Bar, L., Tsiros, I. X., & Hoffman, M. (2012). Passive cooling design options to ameliorate thermal comfort in urban streets of a Mediterranean climate (Athens) under hot summer conditions. [Article]. *Building and Environment*, 57, 110-119. doi: 10.1016/j.buildenv.2012.04.019
- Spagnolo, J., & de Dear, R. (2003). A field study of thermal comfort in outdoor and semi-outdoor environments in subtropical Sydney Australia. *Building and Environment*, 38(5), 721-738. doi: 10.1016/s0360-1323(02)00209-3
- Steane, M. A. (2004). Environmental diversity and natural lighting strategies. In K. Steemers & M. A. Steane (Eds.), *Environmental diversity in architecture* (pp. 3-16). London and New York: Taylor and Francis Group.
- Steemers, K., Ramos, M., & Sinou, M. (2004). Urban diversity. In K. Steemers & M. A. Steane (Eds.), *Environmental diversity in architecture* (pp. 85-100). London and New York: Taylor and Francis Group.
- Su, X., Zhang, X., & Gao, J. (2009). Evaluation method of natural ventilation system based on thermal comfort in China. *Energy and Buildings*, 41(1), 67-70. doi: <http://dx.doi.org/10.1016/j.enbuild.2008.07.010>
- Szokolay, S. V. (2000). Dilemmas of warm humid climate house design. Paper presented at the Proceedings of PLEA 2000 Architecture, City, Environment, Cambridge, England.
- Taleghani, M., Kleerekoper, L., Tenpierik, M., & van den Dobbelsteen, A. (2014). Outdoor thermal comfort within five different urban forms in the Netherlands. *Building and Environment*. doi: 10.1016/j.buildenv.2014.03.014
- Taleghani, M., Tenpierik, M., van den Dobbelsteen, A., & Sailor, D. J. (2014). Heat in courtyards: A validated and calibrated parametric study of heat mitigation strategies for urban courtyards in the Netherlands. *Solar Energy*, 103, 108-124. doi: 10.1016/j.solener.2014.01.033

- Tsiros, I. X., & Hoffman, M. E. (2013). Thermal and comfort conditions in a semi-closed rear wooded garden and its adjacent semi-open spaces in a Mediterranean climate (Athens) during summer. *Architectural Science Review*, 57(1), 63-82. doi: 10.1080/00038628.2013.829021
- Wang, Z., Zhang, L., Zhao, J., & He, Y. (2010). Thermal comfort for naturally ventilated residential buildings in Harbin. *Energy and Buildings*, 42(12), 2406-2415. doi: <http://dx.doi.org/10.1016/j.enbuild.2010.08.010>
- Xiaomin, X., Zhen, H., & Jiasong, W. (2006). The impact of urban street layout on local atmospheric environment. *Building and Environment*, 41(10), 1352-1363. doi: 10.1016/j.buildenv.2005.05.028
- Yang, L. (2003). Climatic analysis techniques and architectural design strategies for bioclimatic design. Xi'an University of Architecture and Technology, Xi'an.
- Ye, X. J., Zhou, Z. P., Lian, Z. W., Liu, H. M., Li, C. Z., & Liu, Y. M. (2006). Field study of a thermal environment and adaptive model in Shanghai. [Research Support, Non-U.S. Gov't]. *Indoor Air*, 16(4), 320-326. doi: 10.1111/j.1600-0668.2006.00434.x
- Zhai, Z., & Previtali, J. M. (2010). Ancient vernacular architecture: characteristics categorization and energy performance evaluation. *Energy and Buildings*, 42(3), 357-365. doi: 10.1016/j.enbuild.2009.10.002
- Zhang, H., Arens, E., Fard, S. A., Huizenga, C., Paliaga, G., Brager, G., & Zagreus, L. (2007). Air movement preferences observed in office buildings. [Research Support, Non-U.S. Gov't Research Support, U.S. Gov't, Non-P.H.S.]. *Int J Biometeorol*, 51(5), 349-360. doi: 10.1007/s00484-006-0079-y
- Zhang, H., & Yoshino, H. (2010). Analysis of indoor humidity environment in Chinese residential buildings. *Building and Environment*, 45(10), 2132-2140. doi: 10.1016/j.buildenv.2010.03.011
- Zuhairy, A. A., & Sayigh, A. A. M. (1993). The development of the bioclimatic concept in building design. *Renewable Energy*, 3(4-5), 521-533.